BIOCHEMISTRY
including biophysical chemistry & molecular biology
Article

Biochemistry **2010,** *49,* 8585–8591 8585
DOI: 10.1021/bi101173c

Transmembrane Segment Packing of the Na^+/Ca^{2+} Exchanger Investigated with Chemical Cross-Linkers†

Xiaoyan Ren, Debora A. Nicoll, Lida Xu, Zhilin Qu, and Kenneth D. Philipson*

Departments of Physiology and Medicine and Cardiovascular Research Laboratories, David Geffen School of Medicine, University of California at Los Angeles, Los Angeles, California 90095-1760

Received July 23, 2010; Revised Manuscript Received August 23, 2010

ABSTRACT: The Na^+/Ca^{2+} exchanger (NCX1) is a plasma membrane protein important in regulating Ca^{2+} in cardiac myocytes. The topological model is comprised of nine transmembrane segments (TMSs). To gain insights into the TMS packing arrangement of NCX1, we performed cysteine cross-linking experiments. Pairs of amino acids in different TMSs were mutated to cysteine on the backbone of a cysteineless NCX1. The mutated exchangers were expressed in an insect cell line and treated with cysteine-specific chemical cross-linkers followed by SDS−PAGE to determine the proximity of the introduced cysteines. Previously, we showed that TMSs 2, 3, 7, and 8 are near one another and that residues in TMSs 1 and 2 are close to TMS 6. In this report, we use the same approach to provide evidence for the arrangement of the remaining three TMSs (4, 5, and 9). We present a computer-generated two-dimensional model of transmembrane packing that minimizes the lengths of all cross-links.

The cardiac Na^+/Ca^{2+} exchanger (NCX1)[1] is an integral membrane protein that extrudes Ca^{2+} from myocardial cells by using the energy of the Na^+ gradient. The exchanger is important in maintaining the balance of Ca^{2+} during cardiac excitation−contraction coupling. Abnormal expression of NCX1 is associated with cardiac malfunction, and NCX1 is a potential therapeutic target for regulation of cardiac function and treatment of disease (*1*, *2*).

In the current topological model (Figure 1), NCX1 is composed of nine transmembrane segments (TMSs) organized in an amino-terminal cluster of five TMSs (N-cluster) and a carboxyl-terminal cluster of four TMSs (C-cluster) connected by a large intracellular loop containing two regulatory Ca^{2+}-binding domains (CBD1 and CBD2) (*3*−*5*). The structures of CBD1 and CBD2 have been resolved, and the key residues for binding regulatory Ca^{2+} are known (*6*−*8*). In contrast, there has been no direct identification of TMS residues that are critical for the binding of transported Ca^{2+} or Na^+ although mutations to some residues can alter Na^+ (*4*, *5*, *9*) or Ca^{2+} (*4*) affinity. To obtain more information about substrate binding and translocation by NCX1, the best approach is to resolve the three-dimensional structure of the full-length protein. This structure, however, remains elusive.

An alternative method for obtaining structural information is the use of disulfide cross-linking to identify residues that are in close proximity (*10*). Santacruz-Toloza et al. (*11*) first noted that a disulfide bond between a residue in the N-cluster with a residue in the C-cluster of NCX1 causes a shift in mobility on SDS−PAGE under nonreducing conditions. Qiu and colleagues (*12*) took advantage of that observation and introduced pairs of cysteines into NCX1 to identify disulfide-induced mobility shifts. They examined the arrangement of TMSs 2, 3, 7, and 8 of NCX1 and found that TMS 7 is close to TMS 3 near the intracellular side of the membrane and is in the vicinity of TMS 2 near the extracellular surface. Also, TMS 2 must adjoin TMS 8. This showed that two functionally important domains in NCX1, the α-1 and α-2 repeats (*13*), are close to each other.

Later, Ren and colleagues (*14*) showed that residues in TMSs 1 and 2 are close to cysteine 768 in TMS 6. Cysteine 768 cross-linked with residues at both ends of TMSs 1 and 2 and is likely located toward the middle of TMS 6. Additionally, NCX1 can form dimers as also identified by cross-linking approaches (*15*). Dimerization occurs along a face of the protein that includes parts of TMS 1 and TMS 2.

In this work, we concentrate on TMSs 4, 5, and 9 and how these TMSs are arranged with respect to the other TMSs. On the basis of all the disulfide cross-linking data, we propose a two-dimensional arrangement for the nine TMSs of NCX1 based on computer modeling.

EXPERIMENTAL PROCEDURES

Construction of Exchanger Cysteine Mutants. Single cysteine mutants were prepared by the QuickChange site-directed mutagenesis method (Agilent Technologies) (*3*). Mutations were generated in 300−500 base pair cassettes and verified by sequencing. Full-length exchangers with single or double mutations were constructed by subcloning the mutated cassettes into the cysteineless exchanger.

†This work was supported by National Institutes of Health Grant HL-49101.

*Corresponding author. Tel: 310-825-7679. Fax: 310-206-7777. E-mail: KPhilipson@mednet.ucla.edu.

[1]Abbreviations: NCX1, Na^+/Ca^{2+} exchanger 1; TMS, transmembrane segment; PAGE, polyacrylamide gel electrophoresis; MTS, methanethiosulfonate; MOPS, 4-morpholinepropanesulfonic acid; CuPhe, $CuSO_4$/phenanthroline; *o*-PDM, *N*′,*N*′-*o*-phenylenedimaleimide; *p*-PDM, *N*′,*N*′-*p*-phenylenedimaleimide; BM(PEG)2, 1,8-bismaleimidodiethylene glycol; 3M, 1,3-propanediyl bismethanethiosulfonate; 6M, 1,6-hexanediyl bismethanethiosulfonate; 8M, 3,6-dioxaoctane-1,8-diyl bismethanethiosulfonate; 11M, 3,6,9-trioxaundecane-1,11-diyl bismethanethiosulfonate; 14M, 3,6,9,12-tetraoxatetradecane-1,14-diyl bismethanethiosulfonate; 17M, 3,6,9,12,15-pentaoxaheptadecane-1,17-diyl bismethanethiosulfonate; NEM, *N*-ethylmaleimide; MTSES, sodium (2-sulfonatoethyl) methanethiosulfonate; WT, wild type; HEK, human embryonic kidney.

Published on Web 08/25/2010

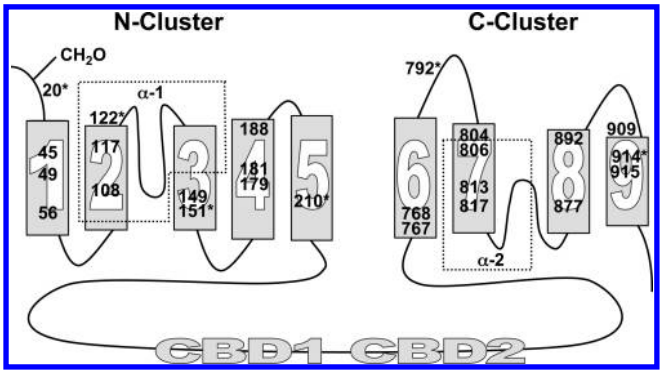

FIGURE 1: Topological model of the cardiac Na^+/Ca^{2+} exchanger and location of amino acids studied in this work. Transmembrane segments are represented by rectangles, the α-repeat regions are surrounded by boxes, and the location of the regulatory Ca^{2+}-binding domains are indicated by "CBD". The predicted locations of the residues mutated to cysteine are shown. Endogenous cysteines of the native exchanger that were reintroduced into the cysteineless NCX1 are indicated with asterisks.

Expression of the NCX1 Cysteine Mutants in Insect High Five Cells. A lepidopteran insect cell expression system BTI-TN-5B1-4 (High Five; Invitrogen) was used for transient transfection of NCX1 cysteine mutants. High Five cells were cultured at 27 °C in Express Five SFM (Invitrogen) supplemented with 20 mM glutamine and 1% penicillin−streptomycin.

Mutant NCX1 cDNAs were subcloned into the pIE1/153A (V4-) triple expression vector (Cytostore), and High Five insect cells were transfected using Cellfectin reagent (Invitrogen). Twenty-four hours posttransfection, Na^+ gradient-dependent $^{45}Ca^{2+}$ uptake into the High Five cells was measured (*12*). Cells were harvested and washed twice with washing buffer (10 mM MOPS, pH 7.4, 140 mM NaCl) and then loaded with Na^+ by incubation with washing buffer containing 1 mM $MgCl_2$, 0.4 mM ouabain, and 25 μM nystatin for 10 min at room temperature. Nystatin was removed from the cells by two washes with washing buffer plus 0.4 mM ouabain. Uptake was initiated by resuspending the cell pellet in assay medium: 10 mM MOPS, pH 7.4, 140 mM KCl (or NaCl as control), 25 μM $CaCl_2$, 0.4 mM ouabain, and 5 μCi/mL $^{45}Ca^{2+}$. After 10 min, the reaction was stopped by adding 1 mL of ice-cold quenching solution (140 mM KCl, 1 mM EGTA) followed by two additional washes with quenching solution. Cell pellets were dissolved in 1 N NaOH at 60 °C for 30 min. Aliquots of samples were subjected to scintillation counting and protein assay (Micro BCA; Pierce).

Cross-Linking in Intact Cells. Intact cells were rinsed with washing buffer, and cross-linking was carried out at room temperature by addition of oxidative reagent (CuPhe), thiol-specific homobifunctional cross-linker (*p*-PDM), maleimide cross-linker BM(PEG)2 (Pierce), or MTS cross-linkers (Toronto Research Chemicals) to the intact cell suspension. The final concentrations of reagents were 1 mM $CuSO_4$ and 3 mM phenanthroline, or 0.5 mM *p*-PDM or BM(PEG)2, or 0.5 mM MTS cross-linkers 2M, 3M, 6M, 8M, 11M, 14M, or 17M. Some samples were preincubated with 10 mM NEM or MTSES. Reactions were terminated after 20 min by addition of NEM (10 mM). Cells were lysed with 1% Triton X-100 plus protease inhibitors (complete, EDTA-free; Roche). Aliquots were subjected to 7.5% SDS−PAGE in the absence of reducing reagents, and immunoblot analysis was carried out with NCX1 antibody R3F1(*16*). All experiments were performed at least three times, and representative data are shown.

Membrane Vesicle Preparation, Cross-Linking, and Vesicular $^{45}Ca^{2+}$ Uptake. Transfected cells were washed twice with washing buffer, resuspended in washing buffer, and homogenized with 10 strokes in a Dounce homogenizer. After centrifugation at 100000*g* for 30 min at 4 °C, the pellet was resuspended in washing buffer. The sample was then passed through a 23-gauge needle 20 times and centrifuged for 5 min at 1258*g* at 4 °C to remove cell debris and nuclei. The supernatant was centrifuged at 100000*g* for 30 min at 4 °C to collect the crude membrane pellet which was resuspended in washing buffer. Cross-linking was induced by the addition of 50 μM 3M or 17M at room temperature for 30 min. Aliquots of the control or cross-linked membrane vesicles were run on SDS−PAGE. Separate aliquots of vesicles were used for $^{45}Ca^{2+}$ uptake. Na^+-dependent Ca^{2+} uptake into vesicles was measured as previously described in detail (*17*). Cross-linked membrane vesicles (5 μL) were washed twice with washing buffer and rapidly diluted into 0.25 mL of uptake medium containing 140 mM KCl (or NaCl for blanks), 0.3 μCi $^{45}Ca^{2+}$, 10 μM Ca^{2+}, 0.4 mM valinomycin, 10 mM MOPS, and pH 7.4, at 37 °C. The uptake reaction was stopped at 3 s with 30 μL of 140 mM KCl and 10 mM EGTA, immediately followed by addition of 1 mL of ice-cold 140 mM KCl and 1 mM EGTA. The vesicles were collected by filtration and washed twice with ice-cold 140 mM KCl and 1 mM EGTA. All experiments were performed in duplicate, with an *n* of 5−11. Data are expressed as means ± SD.

Modeling Helix Packing. Each TMS was reduced to its helical wheel projection of a circle with consecutive amino acids separated by 100° along the circumference of the circle. The nine circles (12 units in diameter) were then rotated and packed into a square of 60 units on a side such as to minimize the total area of the circles that are cut by the cross-links between residues. We included the constraint that TMSs 4 and 5 must be adjacent (due to the short linker between the two). The resulting arrangement of TMSs was then adjusted to minimize the sum of the lengths of the cross-links. For more detail, see Supporting Information.

Hazardous Procedures. All procedures involving the use of $^{45}Ca^{2+}$ were performed under the guidance and following the rules of the Radiation Safety Office at UCLA.

RESULTS

Activity of Paired Cysteine Mutants of NCX1. Single cysteines were first introduced into a cysteineless NCX1 mutant (*12*). NCX1 mutants with two cysteines were then constructed by subcloning and were expressed in insect High Five cells using the pIE1/153A (V4-) triple expression vector. The expression level (both activity and immunoreactive protein) of NCX1 cysteine mutants expressed with this vector was about 50% higher than when expressed with the pIB/V5-His vector used in our previous work (*14*) (data not shown). Only mutants having at least 20% of WT NCX1 activity (Supporting Information Table S1) were selected for cross-linking experiments. The experiments focus on TMSs 4, 5, and 9 (Figure 1) since other TMSs have been investigated previously (*12*, *14*).

Cross-Linkers. We used three different types of cross-linkers. CuPhe is an oxidative reagent, which can catalyze disulfide formation between sulfhydryl groups. The resultant disulfide bond is about 2 Å in length. *p*-PDM and BM(PEG)2 are dimaleimide sulfhydryl cross-linkers that cannot be cleaved by reducing agents. *p*-PDM is a rigid cross-linker with a linker distance of 12 Å and has been used with NCX1 previously (*12*, *14*).

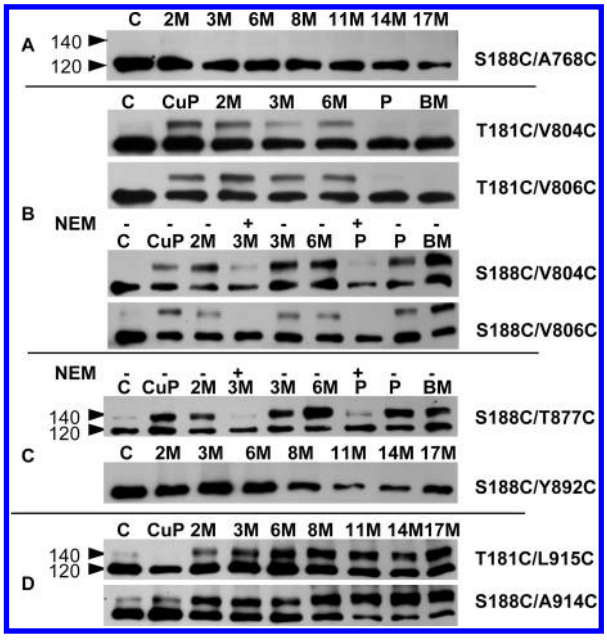

FIGURE 2: Cross-linking between residues in TMS 4 and residues in the C-cluster of TMSs. (A) Cross-linking between TMSs 4 and 6. (B) Cross-linking between TMSs 4 and 7. (C) Cross-linking between TMSs 4 and 8. (D) Cross-linking between TMSs 4 and 9. High Five cells were transfected with the indicated double cysteine mutant cDNAs, and 24 h later, intact cells were treated with cross-linkers as indicated in Experimental Procedures for 20 min at room temperature. Proteins were separated by SDS−PAGE under *nonreducing* conditions, transferred to nitrocellulose membranes, and then probed with an antiexchanger antibody. The presence of a band at 140 kDa indicates cross-linking between the introduced cysteine residues. Some experiments show that preincubation with the membrane permeable reagent NEM blocks subsequent cross-linking. C = control, no cross-linkers added; CuP = CuPhe; P = *p*-PDM; BM = BM(PEG)2.

BM(PEG)2 is more flexible and has a linker distance of 15 Å. MTS cross-linkers react selectively with cysteines, resulting in a disulfide attachment of the spacer group. The MTS reagents we chose are flexible cross-linkers (*18*) including 2M (4 Å), 3M (5 Å), 6M (9 Å), 8M (11 Å), 11M (14 Å), 14M (16 Å), and 17M (21 Å). The appoximate spacer lengths deviate by 1−2 Å (*19*). In control experiments using the mutant S188C/T877C and the cross-linkers 2M, 8M, and 14M at 0.5 mM at room temperature, we found that a 20 min exposure was sufficient to maximize cross-linking (Supporting Information Figure S4). All of the cross-linkers chosen for this study are membrane permeable, and cross-linking experiments were carried out using intact cells unless otherwise specified.

Cross-Linking between Residues in TMS 4 and the C-Cluster of NCX1. *TMS 4 to TMS 6*. Residue 188, modeled to be close to the extracellular side of TMS 4, was paired with residue 767 or 768 in TMS 6. Both S188C/A767C (not shown) and S188C/A768C mutants display wild-type levels of activity (Supporting Information Table S1) but no cross-linking (Figure 2A). Thus, proximity of TMSs 4 and 6 was not detected.

TMS 4 to TMS 7. In previous work (*12*), residues modeled to be near the intracellular sides of TMSs 4 and 7 did not form cross-links. Twelve pairs of cysteine mutants were constructed between TMSs 4 and 7, four of which were active. All four pairs showed mobility shifts upon application of cross-linkers (Figure 2B). Mutants T181C/V804C and T181C/V806C can be cross-linked with thiol reagents 2−9 Å in length but not with the longer bimaleimide cross-linking reagents. S188C/V804C and S188C/V806C could be cross-linked with a greater array of cross-linkers with mobility shifts observed when using cross-linkers with spacer arms between 2 and 15 Å (Figure 2B) or longer (14M and 17M; data not shown). For both mutants containing S188C, cross-linker-induced mobility shifts could be inhibited by preincubation with NEM. On a helical wheel projection of TMS 4 (see Figure 6), residues 181 and 188 are within 20° of each other. In TMS 7, residues 804 and 806 are separated by 160°. These residues are modeled to be near the extracellular surface (Figure 1).

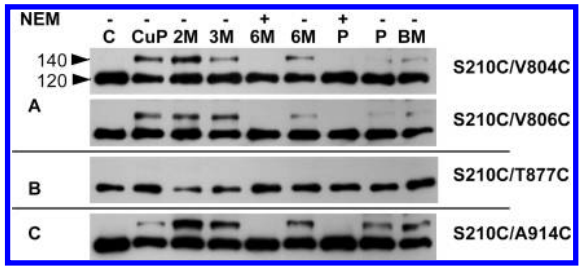

FIGURE 3: Cross-linking between residues in TMS 5 with residues in the C-cluster of TMSs. (A) Cross-linking between TMSs 5 and 7. (B) Lack of cross-linking between TMSs 5 and 8. (C) Cross-linking between TMSs 5 and 9. Experiments were performed as described in Figure 2.

TMS 4 to TMS 8. We paired a cysteine at position 188 (near the extracellular surface) with cysteines at 892 (at the extracellular side) or 877 (toward the intracellular side) in TMS 8. We expected that cross-linking would be more likely to be detected with mutant S188C/Y892C than with S188C/T877C. However, we obtained an unexpected result. Cross-linking was observed in mutant S188C/T877C (Figure 2C) with cross-linkers ranging from 2 to 22 Å in length. Cross-linking was unaffected by the presence or absence of Na^+ in the extracellular medium (Supporting Information Figure S5). No cross-linking was observed with mutant S188C/Y892C (Figure 2C, lower panel).

TMS 4 to TMS 9. Proximity between TMSs 4 and 9 was not observed in previous work utilizing cysteines at positions 909 and 926 toward the ends of TMS 9 (*12*). Thus, we used residues modeled to be more toward the middle of TMS 9. Four mutants were constructed: T181C/S914C, T181C/L915C, S188C/S914C, and S188C/L915C. All were active, and all displayed cross-linking (Figure 2D shows results for T181C/L915C and S188C/S914C), implying that TMSs 4 and 9 are in close proximity.

Cross-Linking between Residues in TMS 5 and the C-Cluster of NCX1. Residue 210 in TMS 5 is a native cysteine. In a previous study, we combined C210 with cysteine residues in the C-cluster of NCX1 but were unable to detect cross-linking (*12*). We chose seven additional residues in TMSs 7, 8, and 9 to pair with residue 210. Of these seven pairs, five were active and four showed mobility shifts upon application of cross-linkers (Figure 3). Cross-linking induced by 6M could be blocked by preincubation with NEM. The results show that TMS 5 is in proximity to TMS 7 and 9.

Cross-Linking between Residues in TMS 9 and the N-Cluster of NCX1. Previously, residues in TMS 9 were paired with residues in TMSs 1−5 (*12*), but none of the active mutants could be cross-linked by CuPhe, *o*-PDM, or *p*-PDM when expressed in HEK293 cells. However, inactive mutant 117/909 did display cross-linking. Thus, we subcloned S117C/K909C and another previously examined mutant, A122C/K909C, into the pIE1/153A (V4-) triple expression vector and expressed them in insect High Five cells (Table 1). No activity was detected with either mutant. We then tried pairing native cysteine 914 or

Table 1: Disulfide Cross-Linking of Exchanger Mutants

C-Cluster		N-Cluster																	
		TMS 1							TMS 2					TMS 3	TMS 4			TMS 5	
		40	41	42	43	45	49	58	59	101	102	106	117	122	151	172	181	188	210
TMS 6	767		+[b]						+[b]									–	
	768		+[b]			+[b]	–[b]	–[a]	+[b]	+[b]	+[b]	–[a]		+[b]	–[a]	–[a]		–	–[a]
	788	–[b]	–[b]		–[a]								–[a]	–[a]				–[a]	
	789		–[b]	–[b]															
TMS 7	804				–[a]								+[a]	–[a]			+	+	+
	806					–	+										+	+	+
	815							–[a]				–[a]			+[a]	–[a]			–[a]
	819							–[a]				–[a]			–[a]	–[a]			–[a]
	821							–[a]				–[a]			+[a]	–[a]			–[a]
	822							–[a]				–[a]			–[a]	–[a]			–[a]
TMS 8	875							–[a]				–[a]			–[a]	–[a]			–[a]
	877					–	+							+	+			+	–
	892	–[b]	–[b]	–[b]	–[a]				–[b]				–[a]	+[a]	+			–	
TMS 9	907	–[b]	–[b]	–[b]					–[b]										
	909	–[b]	–[b]	–[b]	–[a]				–[b]				+[a,c]	–[a]				–[a]	
	912	–[b]	–[b]						–[b]										
	914												–	+	+		+	+	+
	915												+	+	+		+	+	+
	923	–[b]	–[b]	–[b]					–[b]										
	926							–[a]				–[a]			–[a]	–[a]			–[a]

[a]Data published in ref *1*. [b]Data published in ref *2*. [c]Inactive mutant, not included to define packing model. All other data were collected in this work. (−) no cross-linking observed; (+) cross-linking observed; gray shading highlights data used to construct helix-packing model.

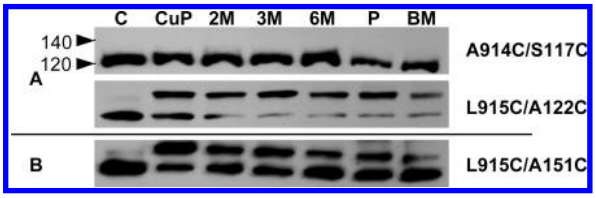

FIGURE 4: Cross-linking between residues in TMS 9 and residues in the N-cluster of TMSs. (A) Cross-linking between TMSs 9 and 2. (B) Cross-linking between TMSs 9 and 3. Experiments were performed as described in Figure 2.

L915C, in the middle of TMS 9, with residues in TMSs 2−5. The 12 mutants we examined all showed Na^+ gradient-dependent Ca^{2+} transport and were then treated with cross-linking reagents. We observed cross-linked product for 11 mutants as determined by decreased electrophoretic mobility. Figure 4 shows results obtained with a negative mutant (A914C/S117C) and two positive mutants (L915C/A122C, L915C/A151C). Our results indicate that TMS 9 is in proximity with TMSs 2, 3, 4, and 5.

Is Residue 877 in TMS 8 Accessible to Residues at the Extracellular Side of the Membrane? Based on a combination of hydropathy analysis, cysteine mutagenesis followed by sulfhydryl modification, immunolocalization, and functional measurements, the exchanger is modeled to have nine transmembrane segments and two re-entrant loops (*3*−*5*) (Figure 1). TMS 8 is modeled to contain 20 amino acids beginning with the intracellular L872 to the extracellular Y892. Thus, residue 877 is modeled to be near the intracellular side of the membrane. That model is supported by results that show nearby residue 875 is accessible to intracellular but not extracellular application of MTSEA (*3*). On the other hand, we observe cross-linking between T877C and S188C (Figure 2C). We did further experiments to confirm the extracellular accessibility of residue 877.

In the wild-type NCX1, residues 20 and 122 are cysteines. C20 is in the amino-terminal loop which is glycosylated (*20*) and clearly extracellular. In the native exchanger, C20 forms a disulfide bond with C792 in the loop between TMSs 6 and 7, which therefore is also extracellular (*11*). C122 is at the extracellular surface of TMS 2. Residue 188 is modeled to be in TMS 4 near the extracellular surface. To confirm that residue 188 is near the outside of the membrane, we paired it with C792. Mutant S188C/A792C showed good cross-linking with 17M (Figure 5A). Treatment with 17M resulted in cross-linking between cysteine 877 and the extracellular cysteines at positions 20, 122, and 188. The relative extents of cross-linking were A20C < A122C < S188C (Figure 5A,B). Preincubation with the membrane-impermeable MTS reagent MTSES or membrane-permeable agent NEM completely blocked cross-linking (Figure 5A). Residue 877 is indeed accessible to the extracellular surface of the membrane.

We also examined the effects of cross-linking on the activity of mutants A20C/T877C, A122C/T877C, and S188C/T877C. In preliminary experiments, we found nonspecific inhibition of cysteineless NCX activity in High Five cells by cross-linking agents (not shown). Therefore, for these experiments, cross-linking and exchanger activity were measured in membrane vesicles prepared from High Five cells. Gels of cross-linked samples using membrane vesicles were similar to those obtained using intact cells (Supporting Information Figure S6). To check if exchanger activity was affected by cross-linking, we first tested the effect of cross-linkers on the activity of the cysteineless exchanger. The cross-linkers 3M and 17M at 50 μM had no significant effect (Figure 5C). With cross-linker 3M, the A20C/T877C exchanger showed no cross-linking (Figure 5B) and no

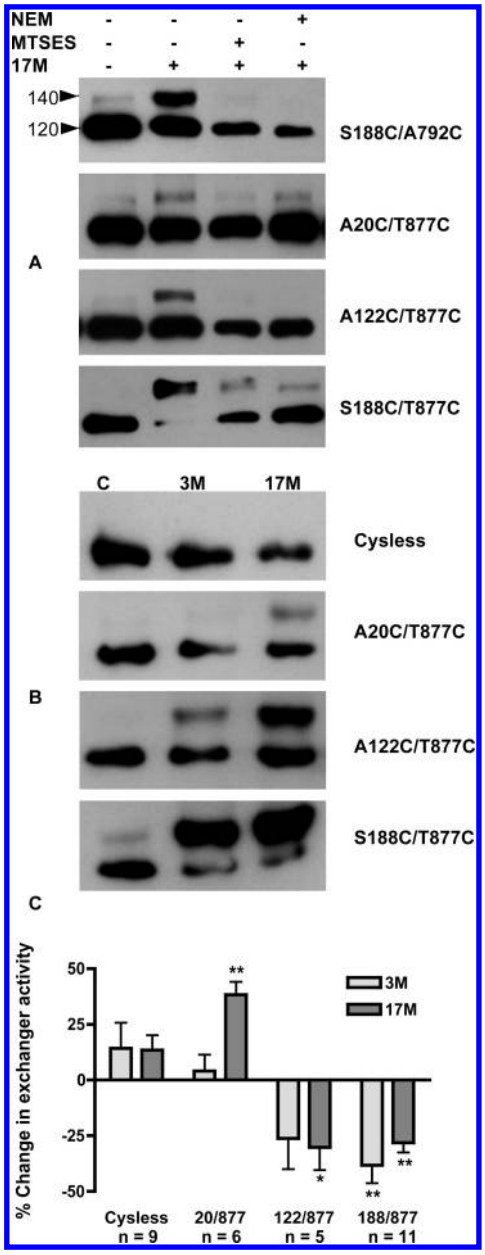

FIGURE 5: Cross-linking between T877C, modeled to be at the intracellular surface of TMS 8, with extracellular residues. (A) The indicated mutants were expressed in High Five cells, preincubated with MTSES or NEM, and then checked for cross-linking with 17M as described in Figure 2. (B) Crude membrane vesicles from transfected insect High Five cells were prepared as described in Experimental Procedures, treated with 50 μM 3M or 17M for 30 min at room temperature, and subjected to SDS−PAGE under nonreducing conditions and transferred to a nitrocellulose membrane for immunoblots. (C) Vesicular exchange activity of the mutants after treatment with 3M or 17M. Data are presented as means ± SD (*t* test; *, $p < 0.05$, or **, $p < 0.01$, as indicated, compared to untreated vesicles; $n = 5-11$ as indicated).

effect on activity (Figure 5C), but 17M cross-linked residues 20C and 877C and stimulated NCX1 activity. For mutant A122C/T877C, 3M and 17M both caused significant cross-linking and inhibition of activity although only the inhibition by 17M was significant (Figure 5C). For mutant S188C/T877C a large fraction of the protein was cross-linked by 3M or 17M (Figure 5B), and both cross-linkers significantly inhibited NCX1 activity. The results suggest that restraining the movements between residues with cross-linkers has modest effects on ion transport. Alternatively, direct modification of the introduced cysteine may be the cause of inhibition, and we cannot eliminate this possibility.

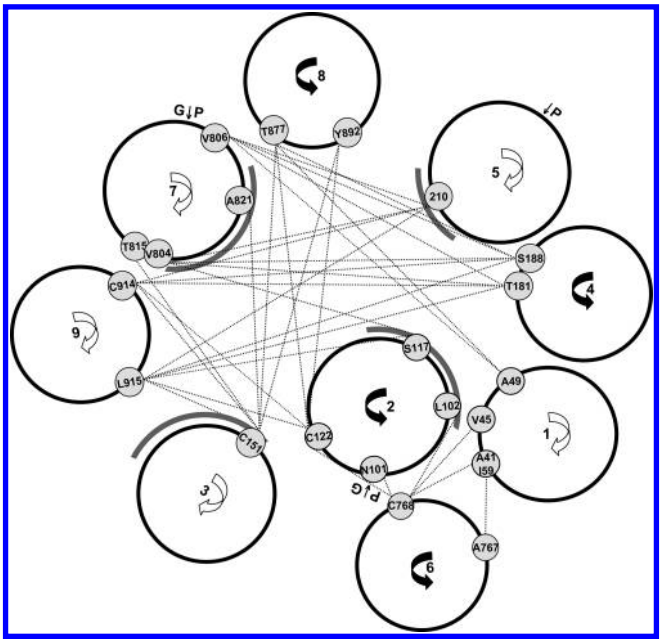

FIGURE 6: Computer-generated model of NCX1 helix packing. All cross-linking data (Table 1) from this and previous work (*12*, *14*) were combined to generate the model. Pairs of residues that demonstrated cross-linking are indicated with lines. The faces of TMSs that contain residues that have altered activity upon mutagenesis are indicated with gray arcs.

Helix Packing of NCX1 Predicted by Computer Modeling. Based on all cross-linking data to date (summarized in Table 1), a helix-packing model for NCX1 was obtained by computer modeling with the following constraints. First, we minimized the sum of the distance between cross-linked residues. Second, we minimized lines connecting cross-linked residues that bisected TMSs. Third, TMS 4 and TMS 5 are constrained to be adjacent because there are only three amino acids between them. The resulting model is shown in Figure 6, and Supporting Information Figure S6 shows the locations of cross-links with an axis perpendicular to the membrane surface. When the pairs of residues that did not form cross-links are mapped onto this model (Supporting Information Figure S7), connecting lines frequently cross through TMSs.

DISCUSSION

We have used a combination of cysteine substitution mutagenesis followed by disulfide cross-linking to gain insights into the helix-packing structure of the TMSs of NCX1. With the results presented here, in combination with two earlier studies, we have observed cross-linking between each of the TMSs of the N-cluster to at least two TMSs in the C-cluster of NCX1 (and vice versa) and are able to present the packing model for NCX1 shown in Figure 6. At best, this arrangement is a two-dimensional slice through the protein.

To obtain our helix-packing model, we use two assumptions: first, that the TMSs are all perpendicular to the membrane and, second, that the TMSs are all continuous α-helices. Neither assumption is likely to be fully accurate. With the growing number of crystal structures of membrane proteins, it is clear that most membrane proteins have TMSs that cross the membrane at an angle. Also, discontinuities in the α-helices are a common

theme, and several transporters have non-α-helical portions of TMSs that are important participants in interactions with substrates (*21*). Prolines in α-helices are one source of discontinuities (*22*), but discontinuities may also occur for other reasons. There are prolines present in TMSs 2 (P112), 5 (P208), and 7 (P813). TMSs 2 and 7 also have a conserved GXXXP motif which places a glycine and proline one helical turn apart, perhaps giving these TMSs considerable flexibility (*23*). With a proline-induced discontinuity, the cross-linked residues 101 and 102 may not be in a strict helical wheel alignment with respect to residues 117 and 122 in TMS 2 as shown in Figure 6. The same would be true for residues 804 and 806 with respect to residues 815 and 821 of TMS 7.

While the cross-linking studies have by no means been exhaustive, it appears that the most "packable" of the TMSs are TMS 2 and TMS 7, both segments of the α-repeats (Figure 1). The α-repeats are regions of sequence similarity that are the apparent result of a gene duplication event. There is much evidence that the α-repeats are critical in the NCX1 transport process. For TMSs 2 and 7 we have observed at least one cross-link with each TMS of the opposite TMS cluster. The packability of TMSs 2 and 7 is predicted by calculating the helix-packing moment for each TMS of NCX1. Helix-packing moments help to identify the packing interfaces in membrane proteins containing multiple transmembrane helices (*24*). In NCX1, TMSs 2 and 7 have 15 and 11 residues with significant packing moments, respectively. No other TMS has more than 6 residues with significant packing moments. Thus, our observations and the prediction agree that TMSs 2 and 7 interact with multiple TMSs and are likely to have fewer interactions with the bilayer.

A number of residues in TMSs 2, 3, 5, and 7 have been implicated in the ion-exchange process of NCX1. Mutations of these residues result in transporters that show no Na^+/Ca^{2+} exchange activity or exchangers with altered ion selectivity/apparent affinities. When mapped onto the TMS helical wheels in our model (gray arcs in Figure 6), these residues are all on interior facing portions of the TMSs. For TMS 2, the helical wheel surface contains three residues (S109, S110, E113) (*13*) that when mutated result in "dead" exchangers and one residue (T103) (*5*) whose mutation results in altered Na^+ affinity and selectivity. In TMS 3, mutants at residues 139, 140, 143, and 147 have either no activity or significantly reduced apparent affinities for Na^+ (*9*). In the helical wheel projection, these residues are all adjacent to C151, which is capable of cross-linking with TMSs 7−9. TMS 5 shares a small amount of sequence similarity to the Na^+ pump, and mutants E199Q and T203 V are inactive (*13*). Those residues are on either side of C210, which can form cross-links with TMSs 7 and 9. Mutations in TMS 7 that result in no Ca^{2+} transport activity are to residues T810, S811, D814, and S818 (*13*). All of these residues map to the same side of the TMS 7 helical wheel defined by cross-linked residues 804 through 821. For TMSs 2 and 7, the arcs that define the regions of residues sensitive to mutagenesis are adjacent to the GXXXP motif. Thus, these functionally important regions may have increased flexibility. In sum, the helix-packing model is independently consistent with mutational analysis in positioning functionally important residues toward the interior of the protein.

The technique we used to determine which residues could form cross-links took advantage of an earlier observation that cross-links between the two clusters of TMSs result in a shift in mobility on SDS−PAGE. This limits the search for proximate residues to interactions between the two TMS clusters, and we are unable to define interactions between TMSs within a cluster. From our helix-packing model, which was generated by minimizing the bisection of helical wheels by cross-links and the sum of the lengths of the cross-links, it appears that there is segregation of the two TMS clusters. The N-cluster is on one side of NCX1 and, with the exception of TMS 6, the C-cluster is on the other side. With that segregation and the inverted topology of the α-repeats, we anticipate that the three-dimensional structure of NCX1 will fit into the growing list of membrane proteins whose TMSs are arranged with a 2-fold symmetry axis perpendicular to the plane of the membrane (*18*).

Especially notable is the accessibility of residue 877. We have previously shown in cysteine-modification experiments that nearby residue 875 is in contact with the cytoplasm (*3*). Here, we show that residue 877 can form cross-links with residues at the extracellular surface over a wide range of cross-linker lengths. This raises some interesting questions regarding the conformation of the NCX1 peptide in this region and/or the conformational changes that can occur here. We propose that residue 877 of TMS 8 is in a region of high flexibility or mobility that permits accessibility to extracellular cross-linking reagents. Perhaps this region is involved in forming the "rocker switch" (*18*) to allow alternating access of Na^+ and Ca^{2+} to either side of the membrane.

All pairs of residues that were used to generate the helix-packing model can be cross-linked with reagents having spacer arms that are 6.5 Å or smaller. Thus, our helix-packing model describes residues that come within at least 6.5 Å of one another. However, the fraction of time that any given pair of residues actually spends in close enough proximity to form cross-links may be quite small. Proteins are dynamic, not rigid, entities that exist in a continuum of conformational states with time scales that vary from femtoseconds to seconds (*25*, *26*). Since our cross-linking reactions were performed at room temperature for 20 min, our results cannot describe a single snapshot of helix packing but rather a number of specific contacts that can occur with different conformations at a near physiologic temperature. We must await a crystal structure for NCX1 to obtain a single snapshot. With that in hand, our cross-linking data may provide insights into some of the movements NCX1 must undergo in a membrane compared to the static structure provided by crystals.

SUPPORTING INFORMATION AVAILABLE

Detailed methods and additional cross-linking data. This material is available free of charge via the Internet at http://pubs.acs.org.

REFERENCES

1. Philipson, K. D., and Nicoll, D. A. (2000) Sodium-calcium exchange: a molecular perspective. *Annu. Rev. Physiol. 62*, 111–133.
2. Blaustein, M. P., and Lederer, W. J. (1999) Sodium/calcium exchange: its physiological implications. *Physiol. Rev. 79*, 763–854.
3. Nicoll, D. A., Ottolia, M., Lu, L., Lu, Y., and Philipson, K. D. (1999) A new topological model of the cardiac sarcolemmal Na^+-Ca^{2+} exchanger. *J. Biol. Chem. 274*, 910–917.
4. Iwamoto, T., Uehara, A., Imanaga, I., and Shigekawa, M. (2000) The Na^+/Ca^{2+} exchanger NCX1 has oppositely oriented reentrant loop domains that contain conserved aspartic acids whose mutation alters its apparent Ca^{2+} affinity. *J. Biol. Chem. 275*, 38571–38580.
5. Doering, A. E., Nicoll, D. A., Lu, Y., Lu, L., Weiss, J. N., and Philipson, K. D. (1998) Topology of a functionally important region of the cardiac Na^+/Ca^{2+} exchanger. *J. Biol. Chem. 273*, 778–783.
6. Nicoll, D. A., Sawaya, M. R., Kwon, S., Cascio, D., Philipson, K. D., and Abramson, J. (2006) The crystal structure of the primary Ca^{2+} sensor of the Na^+/Ca^{2+} exchanger reveals a novel Ca^{2+} binding motif. *J. Biol. Chem. 281*, 21577–21581.
7. Hilge, M., Aelen, J., and Vuister, G. W. (2006) Ca^{2+} regulation in the Na^+/Ca^{2+} exchanger involves two markedly different Ca^{2+} sensors. *Mol. Cell 22*, 15–25.

8. Besserer, G. M., Ottolia, M., Nicoll, D. A., Chaptal, V., Cascio, D., Philipson, K. D., and Abramson, J. (2007) The second Ca^{2+}-binding domain of the Na^{+}/Ca^{2+} exchanger is essential for regulation: crystal structures and mutational analysis. *Proc. Natl. Acad. Sci. U.S.A. 104*, 18467–18472.
9. Ottolia, M., Nicoll, D. A., and Philipson, K. D. (2005) Mutational analysis of the alpha-1 repeat of the cardiac Na^{+}-Ca^{2+} exchanger. *J. Biol. Chem. 280*, 1061–1069.
10. Falke, J. J., and Koshland, D. E., Jr. (1987) Global flexibility in a sensory receptor: a site-directed cross-linking approach. *Science 237*, 1596–1600.
11. Santacruz-Toloza, L., Ottolia, M., Nicoll, D. A., and Philipson, K. D. (2000) Functional analysis of a disulfide bond in the cardiac Na^{+}-Ca^{2+} exchanger. *J. Biol. Chem. 275*, 182–188.
12. Qiu, Z., Nicoll, D. A., and Philipson, K. D. (2001) Helix packing of functionally important regions of the cardiac Na^{+}-Ca^{2+} exchanger. *J. Biol. Chem. 276*, 194–199.
13. Nicoll, D. A., Hryshko, L. V., Matsuoka, S., Frank, J. S., and Philipson, K. D. (1996) Mutation of amino acid residues in the putative transmembrane segments of the cardiac sarcolemmal Na^{+}-Ca^{2+} exchanger. *J. Biol. Chem. 271*, 13385–13391.
14. Ren, X., Nicoll, D. A., and Philipson, K. D. (2006) Helix packing of the cardiac Na^{+}-Ca^{2+} exchanger: proximity of transmembrane segments 1, 2, and 6. *J. Biol. Chem. 281*, 22808–22814.
15. Ren, X., Nicoll, D. A., Galang, G., and Philipson, K. D. (2008) Intermolecular cross-linking of Na^{+}-Ca^{2+} exchanger proteins: evidence for dimer formation. *Biochemistry 47*, 6081–6087.
16. Porzig, H., Li, Z., Nicoll, D. A., and Philipson, K. D. (1993) Mapping of the cardiac sodium-calcium exchanger with monoclonal antibodies. *Am. J. Physiol. 265*, C748–756.
17. Vemuri, R., and Philipson, K. D. (1988) Phospholipid composition modulates the Na^{+}-Ca^{2+} exchange activity of cardiac sarcolemma in reconstituted vesicles. *Biochim. Biophys. Acta 937*, 258–268.
18. Zhou, Y., Guan, L., Freites, J. A., and Kaback, H. R. (2008) Opening and closing of the periplasmic gate in lactose permease. *Proc. Natl. Acad. Sci. U.S.A. 105*, 3774–3778.
19. Loo, T. W., and Clarke, D. M. (2001) Determining the dimensions of the drug-binding domain of human P-glycoprotein using thiol cross-linking compounds as molecular rulers. *J. Biol. Chem. 276*, 36877–36880.
20. Hryshko, L. V., Nicoll, D. A., Weiss, J. N., and Philipson, K. D. (1993) Biosynthesis and initial processing of the cardiac sarcolemmal Na^{+}-Ca^{2+} exchanger. *Biochim. Biophys. Acta 1151*, 35–42.
21. Krishnamurthy, H., Piscitelli, C. L., and Gouaux, E. (2009) Unlocking the molecular secrets of sodium-coupled transporters. *Nature 459*, 347–355.
22. Cordes, F. S., Bright, J. N., and Sansom, M. S. (2002) Proline-induced distortions of transmembrane helices. *J. Mol. Biol. 323*, 951–960.
23. Bright, J. N., and Sansom, M. S. P. (2003) The flexing/twirling helix: exploring the flexibility about molecular hinges formed by proline and glycine motifs in transmembrane helices. *J. Phys. Chem. B 107*, 627–636.
24. Liu, W., Eilers, M., Patel, A. B., and Smith, S. O. (2004) Helix packing moments reveal diversity and conservation in membrane protein structure. *J. Mol. Biol. 337*, 713–729.
25. Henzler-Wildman, K., and Kern, D. (2007) Dynamic personalities of proteins. *Nature 450*, 964–972.
26. Henzler-Wildman, K. A., Lei, M., Thai, V., Kerns, S. J., Karplus, M., and Kern, D. (2007) A hierarchy of timescales in protein dynamics is linked to enzyme catalysis. *Nature 450*, 913–916.